Investigating the oxidation of dimethyl ether/ammonia mixtures by chemical kinetic modeling

Ákos Veres-Ravai[a,b*], István Gyula Zsély[a], Máté Papp[a], Tamás Turányi[a]

[a]Institute of Chemistry, ELTE Eötvös Loránd University, Budapest, Hungary
[b]ELTE Hevesy György PhD School of Chemistry, Budapest, Hungary

Abstract

Nowadays, ammonia (NH_3) is a promising alternative fuel for transportation and power generation. However, the practical application of neat NH_3 is difficult due to its low calorific value, low adiabatic flame temperature, narrow flammability range, and slow burning velocity, therefore, several strategies were implemented to overcome these challenges. Among these strategies, co-firing ammonia with dimethyl ether (DME) has shown promise in increasing the flame velocity and decreasing the ignition delay time of NH_3. DME is also a promising sustainable fuel with net-zero carbon emissions. DME and NH_3 are also well-soluble in each other and form stable mixtures, making their mixtures an attractive alternative fuel option. To facilitate their application, chemical kinetic models are needed that can describe well the combustion of DME/NH_3 mixtures under typical conditions of applications. This work aims to quantitatively compare recent detailed DME/NH_3 combustion mechanisms on a comprehensive experimental data set. Chemical kinetic simulations were performed with the program *Optima++* and solver packages *Cantera* and *OpenSmoke++*. The experimental data (6645 data points in 513 data series from 16 articles) were encoded in ReSpecTh Kinetic Data format v2.5 XML files, covering wide ranges of equivalence ratio, pressure and temperature. The performances of 11 detailed reaction mechanisms were compared quantitatively on a wide range of DME/NH_3 combustion experiments, including concentration measurements in jet-stirred reactor (JSR) and flow reactor (FR), ignition delay time measurements in shock tube (ST) and rapid compression machine (RCM), and laminar burning velocity measurements. The performance of the models in reproducing experimental data was analysed according to experiment types and conditions using quantitative measures. The simulation results for JSR and FR measurements can be sensitive to the temperature used in the calculations, so the effect of experimental temperature uncertainty was also considered. Local sensitivity analysis was performed to identify the most important reactions of the best-performing model. The results of this work can be used in further mechanism development work.

Keywords: ammonia; dimethyl ether; combustion; kinetic modeling; mechanism comparison

*Corresponding author.

1. Introduction

Nowadays, ammonia (NH_3) is a promising alternative fuel for transportation and power generation. However, the practical application of neat NH_3 is difficult due to its low calorific value, low adiabatic flame temperature, narrow flammability range, and slow burning velocity, therefore, several strategies were implemented to overcome these challenges. Among these strategies, co-firing ammonia with dimethyl ether (DME) has shown promise in increasing the flame velocity and decreasing the ignition delay time of NH_3. DME is also a promising sustainable fuel with net-zero carbon emissions. DME and NH_3 are also well-soluble in each other and form stable mixtures, making their mixtures an attractive alternative fuel option.

Due to its increasing importance, several experimental investigations have been carried out, and detailed reaction mechanisms describing the combustion of DME/NH_3 mixtures have been developed in the last two decades. However, the performance of these mechanisms on simulating the experiments is mostly insufficient, and significant discrepancies in the simulation results are obtained. Thus, further investigation and development of these mechanisms are necessary.

In this work, the performance of 11 detailed reaction mechanisms was quantitatively assessed based on how well they can reproduce the results of published experimental data. The method developed by Turányi et al. [2] was used to compare and quantify the performance of the mechanisms. Ignition delay times measured in shock tubes (ST) and rapid compression machines (RCM), and concentration measurements carried out in jet stirred reactors (JSR), flow reactors (FR), as well as laminar burning velocity (LBV) measurements were collected from the available publications. With the best overall model, local sensitivity analysis was performed to identify the most important reactions of the DME combustion process.

2. Experimental data collection

Our aim was to collect a large amount of experimental data on the combustion of DME/NH_3 mixtures. The summary of the experimental data with conditions is given in Table 1. Besides the DME/NH_3 only mixtures, ones containing hydrogen were also included in the present study.

All collected indirect experimental data (6645 data points in 513 data series from 16 articles) were encoded in ReSpecTh Kinetics Data (RKD) files.

The RKD format [3] is XML-based and can be read well by both humans and computer programs. The RKD-format files were created with our Optima++ code [4]. *Optima++* was also used for reading the data files, running *Cantera* [5] and *OpenSMOKE++* [6], which were the two solvers used in the study, and comparing the simulation results with the experimental data.

Table 1 The collected experimental data and the experimental conditions. Abbreviations and notations: FR: flow reactor; JSR: jet-stirred reactor; ST: shock tube; RCM: rapid compression machine; c_{out}: outlet concentration; IDT: ignition delay time; LBV: laminar burning velocity *T*: (cold-side) temperature; *p*: pressure; φ: equivalence ratio

Experimental method	Measured data	# of data points / data series / XMLs	*T* / K	*p* / atm	φ
FR	c_{out}	3193/269/27	173 – 1423	0.99 – 39.48	0.39 – 1.88
JSR	c_{out}	2689/127/12	450 – 1260	1.00	0.50 – 2.00
ST	IDT	132/18/18	689 – 1983	1.10 – 11.90	0.50 – 2.00
RCM	IDT	292/45/45	622 – 1027	4.68 – 69.97	0.50 – 2.00
Laminar flames	LBV	339/54/54	298 – 423	0.99 – 5.00	0.04 – 3.40

3. Comparison of the performance of the mechanisms

The experimental data were reproduced using recent detailed reaction mechanisms that were developed to describe the combustion of DME/NH_3 mixtures. All collected experimental data were simulated with each reaction mechanism. *Cantera* was used primarily as a solver for the simulations, while *OpenSmoke++* was used to simulate flow reactor measurements.

The obtained simulation results, belonging to different mechanisms, were typically different from each other and sometimes also from the experimental data. Two typical examples of the behaviour of the mechanisms can be seen in Figure 1.

Agreement of the simulation results with the experimental data was investigated comprehensively using the following error function:

$$E = \frac{1}{N}\sum_{f=1}^{N_f}\sum_{s=1}^{N_{fs}}\frac{1}{N_{fsd}}\sum_{d=1}^{N_{fsd}}\left(\frac{Y_{fsd}^{\mathrm{sim}} - Y_{fsd}^{\mathrm{exp}}}{\sigma(Y_{fsd}^{exp})}\right)^2 \qquad (1)$$

In equation (1), N is the number of experimental data series in the data collection, N_f is the number of datasets (i.e. the number of RKD files), N_{fs} is the number of data series in dataset f, and N_{fsd} is the number of data points in data set f and data series s. y_{fsd}^{sim} and y_{fsd}^{exp} are the simulated and experimental values of the d-th experimental data point of the s-th data series in the f-th dataset. $\sigma(Y_{fsd}^{\mathrm{exp}})$ is the estimated standard deviation of the data point y_{fsd}^{exp}. The

corresponding simulated value y_{fsd}^{sim} is obtained from a simulation using a detailed mechanism and an appropriate simulation method. If a measured value is characterized by absolute errors (the scatter is independent of the magnitude of y_{fsd}), then $Y_{fsd} = y_{fsd}$. If the experimental results are described by relative errors (the scatter is proportional to the value of y_{fsd}), then option $Y_{fsd} = \ln(y_{fsd})$ is used.

When estimating the standard deviation of the data points, both uncertainty $\sigma_{\mathrm{exp,fsd}}$ provided by the authors of the publications or estimated in this study, and the $\sigma_{\mathrm{stat},i}$ statistical scatter of the data points were considered:

$$\sigma_{fsd} = \sqrt{\sigma_{\mathrm{exp},fsd}^2 + \sigma_{\mathrm{stat},fs}^2} \qquad (2)$$

For the flow reactor and jet-stirred reactor measurements, the measured temperature values are uncertain, and the simulation results can be sensitive to the temperature used in the calculations, so the effect of experimental temperature uncertainty was also considered. When estimating the standard deviation of the data points, an additional $\sigma_{unc,fsd}^2$ variance term, calculated using the error propagation formula, was added to Equation (2) to consider the experimental temperature uncertainty:

$$\sigma_{fsd} = \sqrt{\sigma_{\mathrm{exp},fsd}^2 + \sigma_{\mathrm{stat},fs}^2 + \sigma_{\mathrm{unc},fsd}^2} \qquad (3)$$

The performance of a mechanism can be considered good if $E < 9$ is fulfilled, which means the experimental values were reproduced within the 3σ standard deviation limits of the data series on average. The error function values calculated using all the experimental data and some subsets based on the experiment types are shown in Table 2.

The table, however, does not contain all the collected data points. To avoid biased conclusions, those points were excluded from comparison, for which the error function value was greater than 9 for all models, indicating that no mechanism could simulate them properly. Those data points for which the simulations failed due to some mechanistic error were also excluded. The number of failed simulations, along with the remaining data points, are also shown in Table 2. As can be seen, the number of failed simulations is especially high for Shrestha-2021, but it is still negligible compared to the number of all collected data.

As can be seen in Table 2, the overall best-performing mechanism is Issayev-2022. It is, however, only under the desirable E value ($E = 9$) for the shock tube and LBV experiments. In general, most mechanisms perform worse than this for most experiment types. Jiang-2024 and Zhu-2023 are the second and third best models, respectively, with overall E values under 40, and two more mechanisms are under 60.

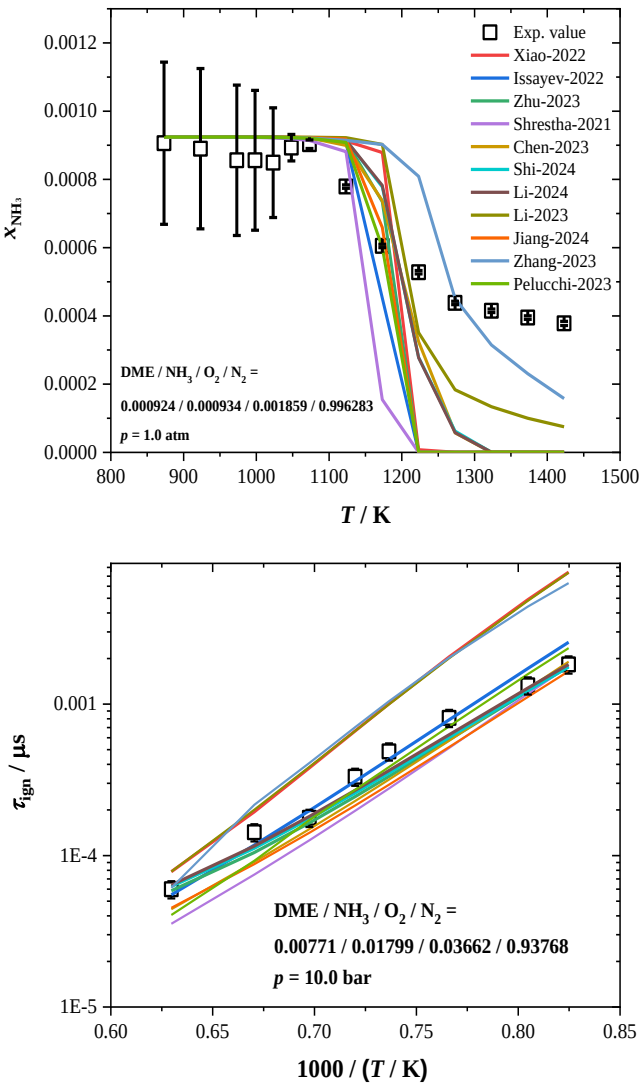

Figure 1 Comparison of the experimental values measured in homogenous reactors and the corresponding simulation results in the case of two example datasets. a) simulation of an FR outlet concentration measurement by Ruíz-Gutíerrez et al. [7]; b) simulation of ignition delay times measured in a shock tube by Jin et al. [8].

Table 2 Comparison of the investigated reaction mechanisms based on the error function values calculated for all experimental data and various subsets of them. The final order in this table is based on the overall error function values. The number of unsuccessful simulations is also indicated.

		JSR	FR	ST	RCM	LBV	Overall	Failed
Number of data series		127	269	17	44	46	1210	
Number of data points		2465	2789	108	260	204	5826	
Issayev-2022	[9]	65.5	37.3	8.7	24.7	5.5	22.2	23
Jiang-2024	[10]	46.5	7.7	150.9	20.7	11.6	32.4	6
Zhu-2023	[11]	23.1	14.4	131.1	33.1	19.2	35.6	8
Pelucchi-2023	[12]	33.2	12.6	58.3	97.3	35.0	52.0	44
Chen-2023	[13]	104.7	30.4	250.5	25.6	26.5	59.0	6
Shrestha-2021	[14]	802.1	34.7	54.4	66.3	42.6	111.2	68
Shi-2024	[15]	388.4	10.4	650.0	59.3	11.9	129.5	14
Li-2024	[16]	393.6	10.2	648.6	62.7	11.6	130.7	10
Zhang-2023	[17]	1129.2	48.2	435.4	41.9	19.2	169.0	10
Li-2023	[18]	317.7	36.8	550.7	389.5	129.0	253.3	6
Xiao-2022	[19]	266.1	38.4	335.9	1436.1	8.0	496.7	7

As these are the lowest values, the results also indicate that the mechanisms cannot reproduce the experimental data within their 3σ uncertainty range on average, meaning that further development of the models is necessary.

It is also useful to use stacked bar plots of errors to compare the mechanisms. This can be seen in Figure 2, where the distribution of the error function values is visualized. It shows the frequencies of the data points that were reproduced by the mechanisms within a given threshold of the multiple of the estimated standard deviation. Here, the error function values were not considered, only the count of them within the thresholds. Therefore, it resulted in a different order than Table 2 based on the average error function value.

The stacked bar plot shows that there are no great differences between the mechanisms in the percentages as they reproduce the data points in different uncertainty ranges. Based on this comparison, Jiang-2024 performs the best with reproducing 85.1% of the data points within 3σ uncertainty. Issayev-2022, the best model by average overall E value is the second one with 83.8%, while Zhu-2023 is the third one with 83.4%. The results show that most data points considered in the comparison are reproduced within the desirable uncertainty range, however, about 15% percent of the data points are not even for the best model (this is 28% for the worst one), and these lead to the high average values in Table 2. In a model optimization work, it would be desirable to improve the description of these data points as well.

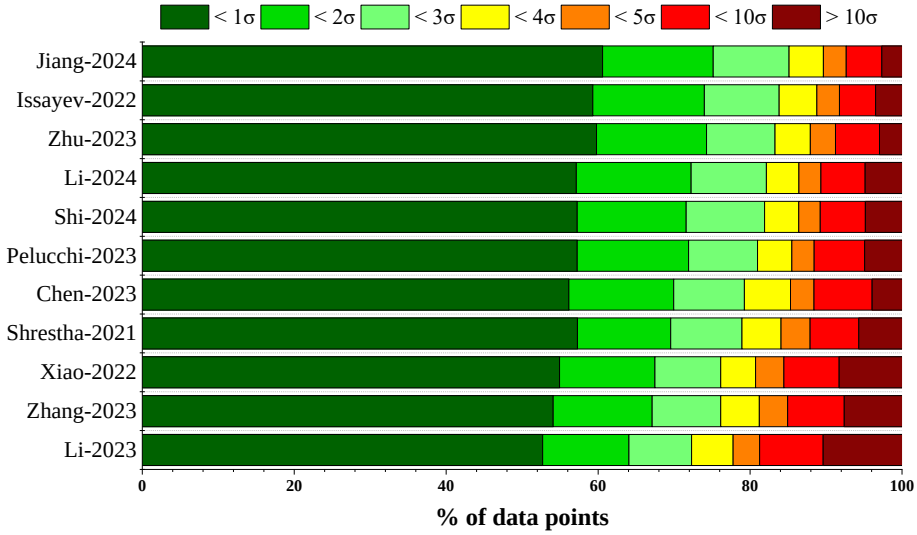

Figure 2 Stacked bar plot of the frequencies of the reproduction of data points within given multiples of the estimated standard deviations of the data. The final order in the figure is based on the "$< 3\sigma$" values.

4. Results of the sensitivity analysis

Local sensitivity analysis [20] was carried out with the Issayev-2022 mechanism using 911 data points to identify the most important reactions in the best-performing model. The analysis was carried out only for the outlet concentration and ignition delay time measurements. For the flow reactor and jet-stirred reactor experiments, only the concentration changes of DME and NH_3 were considered. For the ignition delay time measurements, we experienced high running times for several XMLs and due to this, fewer experimental data points were chosen from these files to complete the sensitivity analysis.

The sensitivity coefficients of the measured values with respect to the +5% relative perturbation of *A* preexponential Arrhenius parameters for each reaction were investigated. Table 3 shows the first 10 reactions with the highest frequencies of significant sensitivity from the considered mechanism for each experiment type investigated. For the outlet concentration measurements, the results are presented according to species. A sensitivity coefficient is considered significant if its normalized absolute value is greater than 10% of the highest absolute normalized sensitivity coefficient of this data point. The frequency values (the freq. columns in Table 3) show the ratio of these important data points to all data points. The $|\widetilde{sn}|_j$ values in Table 3 are the mean scaled absolute normalized sensitivity coefficients:

$$|\widetilde{sn}|_j = \frac{1}{N_i}\sum_{i=1}^{N_i}\frac{|sn_{ij}|}{\max|sn|_i} \qquad (4)$$

Here *i* is the index of the data point and *j* is the index of the reaction (*A* parameter) in the mechanism. The scaling of the normalized sensitivity coefficients described with Equation (4) was done by dividing with the maximum sensitivity coefficient of the data point.

Based on the sensitivity analysis results of Table 3, the most important reactions of Issayev-2022 are dependent on the experiment type and the investigated species when DME and NH_3 are considered separately, however, there are certain reactions that are present for most types and both species. There are reaction steps from the DME oxidation system, the ammonia oxidation system, there are reactions between species connected to the ammonia system with DME and hydrocarbons, and also from the core hydrogen system. The reaction of ammonia with the hydroxyl racidal, NH_3+OH=NH_2+H_2O is between the top 2 reactions in all cases and in the top 10 for the shock tube experiments. There are other important reactions of amino radical in several cases, including the one in which it reacts with DME: CH_3OCH_3+NH_2 = CH_3OCH_2+NH_3, which is especially important for the concentration change of NH_3 in flow reactor. Reactions of the nitrogen-free DME oxidation system are also very significant based on the sensitivity analysis. The reaction of DME with the hydroxyl radical, CH_3OCH_3+OH=CH_3OCH_2+H_2O of high importance for the concentration change of DME in jet-stirred reactor and for the RCM experiments where this is the first on the list, but it is present for other cases as well, except for the shock tube experiments. The unimolecular decomposition of DME, CH_3OCH_3+M = CH_3+CH_3O+M and its low-pressure limit reaction are also very important in most cases, especially for the flow reactor and the shock tube experiments, while the reaction of DME with the hydroperoxyl radical, CH_3OCH_3+HO_2 = CH_3OCH_2+H_2O_2 and the hydrogen radical, CH_3OCH_3+H = CH_3OCH_2+H_2, are also important in some cases. Some reactions including formaldehyde or formyl radical also appear between the most important reactions for several experiment types, e.g. HCO+M=H+CO+M, but they are not as important as for a neat DME system. The lists also contain one reaction from the core subsystems, like the combustion of hydrogen, though in a smaller extent in comparison with other fuels like neat methane, methanol, ethanol or butanol where usually the O_2+H=O+OH is the most sensitive reaction. Here this only stands for the shock tube measurements, but it is also present between the 10 most important reactions for all other cases, except for the RCM experiments. No other reactions from this subsystem are present. Some reactions of methyl radical were also important, e.g. CH_3+O_2=CH_2O+OH and CH_3+CH_3+M=C_2H_6+M, especially for the reactor measurements.

For the flow reactor and jet-stirred reactor experiments, the most important reaction steps are mainly from the DME oxidation subsystem, even for the concentration change of NH_3, though reactions of nitrogen-containing species also appear. For the shock tube experiments, the picture is mixed with reactions from several subsystems, while for the RCM experiments, there are mostly reactions from the ammonia and NOx subsystems. These differences are due to the different nature of experiment types and the different condition intervals the measurements covered.

The most important reactions identified in this study are mostly in accordance with the results obtained by other researchers that performed local sensitivity analysis on the combustion of DME/NH_3 mixtures [21-22]. The results can be used in further mechanism optimization work.

Table 3 Comparison of the sensitivity analysis results of the *A* preexponential factors of the 10 most sensitive reactions of the Issayev-2022 mechanism by experiment type. Freq.: The percentage number when the reaction had higher absolute sensitivity coefficient than 10% of the largest absolute sensitivity coefficient of the given data point. In parenthesis: the overall number of data points used for the sensitivity analysis. $|\widetilde{sn}|_j$: mean of the scaled normalized absolute sensitivity coefficients. (LP): low pressure limit. (DUP): the given set of the duplicate Arrhenius-parameters.

	FR-NH_3			FR-DME		
		freq. (%) (285)	$\lvert\widetilde{sn}\rvert_j$		freq. (%) (290)	$\lvert\widetilde{sn}\rvert_j$
1.	NH_3+OH = NH_2+H_2O	57.9	0.292	CH_3OCH_3+M = CH_3+CH_3O+M	61.8	0.415
2.	CH_3OCH_3+NH_2 = CH_3OCH_2+NH_3	49.3	0.343	NH_3+OH = NH_2+H_2O	53.3	0.232
3.	CH_3OCH_3+M = CH_3+CH_3O+M	45.2	0.318	CH_3OCH_3+M = CH_3+CH_3O+M (LP)	51.6	0.281
4.	CH_3+CH_3+M = C_2H_6+M	44.8	0.213	CH_3+CH_3+M = C_2H_6+M	51.2	0.167
5.	O_2+H = OH+O	42.4	0.229	CH_3+O_2 = CH_2O+OH	50.9	0.188
6.	CH_3+NH_2 = CH_3NH_2	41.4	0.234	CH_3OCH_3+CH_3 = CH_3OCH_2+CH_4	50.5	0.308
7.	CH_3OCH_3+OH = CH_3OCH_2+H_2O	41.4	0.233	CH_3OCH_3+OH = CH_3OCH_2+H2O	42.5	0.226
8.	CH_3OCH_3+H = CH_3OCH_2+H_2	41.4	0.172	CH_3OCH_3+NH_2 = CH_3OCH_2+NH_3	36.1	0.212
9.	CH_3OCH_3+M = CH_3+CH_3O+M (LP)	39.0	0.224	CH_3+CH_3+M = C_2H_6+M (LP)	34.4	0.088
10.	NH_2+NO = N_2+H_2O	37.6	0.190	O_2+H = OH+O	33.0	0.178
	JSR-NH_3	(90)		JSR-DME	(90)	
1.	NH_3+OH = NH_2+H_2O	78.9	0.482	CH_3OCH_3+OH = CH_3OCH_2+H_2O	88.9	0.473
2.	NH_2+HO_2 = H_2NO+OH	61.1	0.206	NH_3+OH = NH_2+H_2O	81.1	0.389
3.	CH_3+O_2 = CH_2O+OH	54.4	0.302	CH_3OCH_3+HO_2 = CH_3OCH_2+H_2O_2	64.4	0.191
4.	CH_3OCH_2+O_2 => CH_2O+CH_2O+OH	53.3	0.115	CH_3OCH_3+NH_2 = CH_3OCH_2+NH_3	53.3	0.313
5.	O_2+H = OH+O	52.2	0.374	CH_3OCH_3+H = CH_3OCH_2+H_2	52.2	0.326
6.	CH_3OCH_3+OH = CH_3OCH_2+H_2O	51.1	0.213	CH_3+O_2 = CH_2O+OH	51.1	0.254
7.	CH_3OCH_2+O_2 = $CH_3OCH_2O_2$	50.0	0.163	NH_2+NO = N_2+H_2O	51.1	0.214
8.	CH_3OCH_2 = CH_3+CH_2O	48.9	0.284	CH_3OCH_2 = CH_3+CH_2O	48.9	0.236
9.	CH_4+O_2 = CH_3+HO_2	48.9	0.197	CH_4+O_2 = CH_3+HO_2	48.9	0.196
10.	HCO+M = H+CO+M (LP)	48.9	0.172	O_2+H = OH+O	47.8	0.295
	IDT-RCM	(70)		IDT-ST	(86)	
1.	CH_3OCH_3+OH = CH_3OCH_2+H_2O	100.0	0.747	H+O_2 = O+OH	95.3	0.745
2.	NH_3+OH = NH_2+H_2O	100.0	0.730	CH_3OCH_3+M = CH_3O+CH_3+M (LP)	83.7	0.456
3.	CH_3OCH_3+HO_2 = CH_3OCH_2+H_2O_2	100.0	0.588	CH_3OCH_3+M = CH_3O+CH_3+M	80.2	0.338
4.	CH_3OCH_3+NH_2 = CH_3OCH_2+NH_3	100.0	0.519	CH_3+HO_2 = CH_3O+OH	77.9	0.242
5.	NH_2+NO = NNH+OH	100.0	0.460	HCO+M = H+CO+M	68.6	0.246
6.	$CH_3OCH_2O_2$ = $CH_2OCH_2O_2H$	100.0	0.282	CH_3OCH_3+H = CH_3OCH_2+H_2	67.4	0.182
7.	CH_2O+NH_2 = HCO+NH_3	98.6	0.494	NH_3+H = NH_2+H_2	53.5	0.250
8.	NH_2+NO_2 = N_2O+H_2O	97.1	0.330	CH_2O+NH_2 = HCO+NH_3	52.3	0.357
9.	H_2NO+O_2 = HNO+HO_2	95.7	0.607	HCO+O_2 = CO+HO_2	52.3	0.183
10.	NH_2+NO = N_2+H_2O	95.7	0.600	NH_3+OH = NH_2+H_2O	52.3	0.156

5. Conclusions

In the present study, 6645 data points in 513 data series of 16 experimental articles corresponding to the combustion of dimethyl ether/ammonia mixtures and also the ones containing hydrogen as well, were collected form the literature and simulated using 11 detailed reaction mechanisms with *Cantera* and *OpenSMOKE++* using simulation framework *Optima++*. The simulation results of different mechanisms were typically different from each other and from experimental data in several cases. The mechanism Issayev-2022 had the best performance followed by Jiang-2024 and Zhu-2023. No mechanism could reproduce overall experimental data within their 3σ uncertainty range on average, which means that more development of them is necessary. The error distributions showed that most data points (about 72-85%) could be reproduced within this range by the models, and the remaining 15-28% led to these high averages. Local sensitivity analysis was carried out with the best-performing Issayev-2022 using 911 data points. The most important reactions were investigated by experiment types and according to DME and NH_3 for the outlet concentration measures and showed differences according to experiment type and the species investigated. The most important steps include reactions from the individual DME and NH_3 oxidation systems and reactions of DME species with NH_3 species. For most experiments, the most

important reactions are in accordance with the findings of other authors.

Declaration of competing interest

The authors declare that they have no known competing financial interests or personal relationships that could have appeared to influence the work reported in this paper.

Acknowledgements

The authors acknowledge the support of the NKFIH grant OTKA K147024 of the Hungarian National Research, Development and Innovation Office and CYPHER CA22151 COST Action, which is supported by COST (European Cooperation in Science and Technology). ÁVR was supported by the DKOP-23 Doctoral Excellence Program of the Ministry for Culture and Innovation of Hungary from the source of the National Research, Development, and Innovation Fund.

References

[1] C. Arcoumanis, C. Bae, R. Crookes, E. Kinoshita, The potential of di-methyl ether (DME) as an alternative fuel for compression-ignition engines: A review, Fuel 87 (2008), 1014-1030.

[2] T. Turányi, T. Nagy, I. G. Zsély, M. Cserháti, T. Varga, B. T. Szabó, I. Sedyó, P. T. Kiss, A. Zempléni, H. J. Curran, Determination of rate parameters based on both direct and indirect measurements, Int. J. Chem. Kinet. 44 (2012) 284–302.

[3] T. Varga, C. Olm, M. Papp, Á. Busai, A. Gy. Szanthoffer, I. Gy. Zsély, T. Nagy, T. Turányi, ReSpecTh Kinetics Data Format Specification v2.5, Chemical Kinetics Laboratory, ELTE Institute of Chemistry (2024).

[4] M. Papp, T. Varga, Á. Busai, I. Gy. Zsély, T. Nagy, T. Turányi: Optima++ v2.5: A general C++ framework for performing combustion simulations and mechanism optimization (2024); available at http://respecth.hu/ (Accessed March 2025).

[5] D. G. Goodwin, H. K. Moffat, I. Schoegl, R. L. Speth, B. W. Weber. Cantera: An object-oriented software toolkit for chemical kinetics, thermodynamics, and transport processes (2023). https://www.cantera.org (Accessed March 2025).

[6] A. Cuoci, A. Frassoldati, T. Faravelli, E. Ranzi, OpenSMOKE++: An object-oriented framework for the numerical modeling of reactive systems with detailed kinetic mechanisms, Comput. Phys. Commun. 192 (2015) 237–264.

[7] A. Ruiz-Gutiérrez, P. Rebollo, M.U. Alzueta, Combustion of NH3/DME and NH3/DME/NO mixtures, Fuel 381 (2025) 133253.

[8] Y. Jin, X. Li, X. Wang, Z. Ma, X. Chu, Effect of dimethyl ether on ignition characteristics of ammonia and chemical kinetics, Fuel 343 (2023) 127885.

[9] G. Issayev, B. R. Giri, A. M. Elbaz, K. P. Shrestha, F. Mauss, W. L. Roberts, A. Farooq, Ignition delay time and laminar flame speed measurements of ammonia blended with dimethyl ether: A promising low carbon fuel blend, Renewable Energy 181 (2022) 1353-1370.

[10] X. Jiang, Q. Zhang, X. Liu, T. Zhang, Y. Zhang, Z. Huang, F. Deng, N. Zhao, H. Zheng, Y. Yan, A shock tube study of the ignition delay time of DME/ammonia mixtures: Effect of fuel blending from high temperatures to the NTC regime, Fuel 367 (2024) 131426.

[11] S. Zhu, Q. Xu, R. Tang, J. Gao, Z. Wang, J. Pan, D. Zhang,A comparative study of oxidation of pure ammonia and ammonia/dimethyl ether mixtures in a jet-stirred reactor using SVUV-PIMS, Combust. Flame 250 (2023) 112643.

[12] M. Pelucchi, S. Schmitt, N. Gaiser, A. Cuoci, A. Frassoldati, H. Zhang, A. Stagni, P, Oßwald, K. Kohse-Höinghaus, T. Faravelli, On the influence of NO addition to dimethyl ether oxidation in a flow reactor, Combust. Flame 257 (2023) 112464.

[13] J. Chen, X. Gou, Experimental and kinetic study on the extinction characteristics of ammonia-dimethyl ether diffusion flame, Fuel 334 (2023) 126743.

[14] K. P. Shrestha, C. Lhuillier, A. A. Barbosa, P. Brequigny, F. Contino, C. Mounaïm-Rousselle, L. Seidel, F. Mauss, An experimental and modeling study of ammonia with enriched oxygen content and ammonia/hydrogen laminar flame speed at elevated pressure and temperature, Proc. Comb. Inst. 38 (2021) 2163-2174.

[15] X. Shi, W. Li, J. Zhang, Q. Fang, Y. Zhang, Z. Xi, Y. Li, Exploration of NH_3 and NH_3/DME laminar flame propagation in O2/CO2 atmosphere: Insights into NH3/CO2 interactions, Combust. Flame 260 (2024) 113245.

[16] Y. Li, Y. Zhang, J. Fang, Z. Xi, J. Zhang, Z. Liu, X. Shi, W. Li, Combustion enhancement of ammonia by co-firing dimethyl ether/hydrogen mixtures under methane-equivalent calorific value, Combust. Flame 265 (2024) 113490.

[17] Y. Zhang, Q. Wang, L. Dai, M. Zhang, C. Yu, Numerical Study on the Combustion Properties of Ammonia/DME and Ammonia/DMM Mixtures, Energies 16 (2023) 6929.

[18] H. Li, H. Xiao, Effect of H2 addition on laminar burning velocity of NH_3/DME blends by experimental and numerical method using a reduced mechanism, Combust. Flame 257 (2023) 113000.

[19] H. Xiao, H. Li, Experimental and kinetic modeling study of the laminar burning velocity of NH_3/DME/air premixed flames, Combust. Flame 245 (2022) 112372.

[20] T. Turányi, A. S. Tomlin, Analysis of Kinetic Reaction Mechanisms; Springer, 2014.

[21] M. Li, K. Moshammer, Comparison of the effects of adding the isomers ethanol or dimethyl ether on ammonia oxidation chemistry Fuel 384 (2025) 133907.

[22] P. García-Ruiz, P. Ferrando, M. Abián, M. U. Alzueta, High-pressure conversion of ammonia additivated with dimethyl ether in a flow reactor, Combust. Flame 272 (2025) 113875.